The Service State Behavior of Reinforced Concrete Membrane Elements using Rotating Crack Model


Bhang, Jee-Hwan* Kang, Won-Ho**

ABSTRACT

A theory is proposed to predict the response of the load-deformation relationship of the reinforced concrete structures under the service state after cracking. The crack direction and concrete strains through the loading history before failure can be estimated by this theory based on the rotating crack model, which considers equilibrium, compatibility conditions, and average stress-strain relationship. The proposed crack direction and deformation show good agreement with test results under service state. The behavior of a variety of concrete structures, such as shear walls, deep beams and the web of box girders, can be predicted by this proposed theory under service state.

Keywords : reinforced concrete membrane element, service state, orthogonal reinforcement, rotating crack model, smeared crack, average stress, crack direction

*Lecturer, Dept. of Civil and Ocean Engineering Dong-A University, Korea
**KCI member, Professor, Dept. of Civil and Ocean Engineering Dong-A University, Korea

1. INTRODUCTION

Reinforced concrete wall-type and shell-type structures, such as the web of box girders, shear walls, nuclear containment vessels, and concrete offshore structures, can be considered as an assembly of membrane elements subjected to two in-plane normal stresses and an in-plane shear stress. In this study a rotating crack model is used to predict nonlinear response of such membrane elements. This rational model is based on the four fundamental principles of the mechanics of materials: 1) stress equilibrium, 2) strain compatibility, 3) load-deformation response of cracked member, and 4) constitutive laws for material. This model can predict not only the shear strength but also shear load-deformation responses of a structure at service state.

The rotating crack model has been developed by Gupta and Akbar[1], and is usually presented in a total strain formulation. This model has been used in the analysis of reinforced concrete structures. The mechanical model of Kolleger[2], Crisfield and Wills[3], Vecchio and Collins[4], and Hsu[5] are based on the rotating crack model, where the concrete struts are assumed to orient at an angle in the principal direction[2-5]. The change in the crack direction and the consequential change in direction of the maximum stiffness were clearly observed in the experiments of Vecchio and Collins, Bhide and Collins, Kolleger and Mehlhorn, and Pang and Hsu[6-9].

The basic assumption for Rotating Crack Model is that a succession of cracks develops in increasingly divergent directions in concrete under the incremental monotonic loading. The direction of the first crack is determined by the direction of the principal tensile stresses in elastic analysis. After the first cracking, the change in direction of the subsequent cracks occurs according to the changes in the direction of the principal tensile stresses in the concrete, which are dependent on the relative amount of steel in the longitudinal and transverse directions.

In this rotating crack model, reinforced concrete is treated as a continuous material with "smeared cracks" ,so that the principle of transformation of the stresses and strains, represented graphically by Mohr's circle, can be applied. Constitutive laws are based on average stresses and strains. The average stress of a reinforcing bar, or the average stress of concrete in tension, means the average of the stresses from a crack to the adjacent point where bond stress is zero.

An analytical method is proposed in this study to calculate the crack directions and the shear load-deformation responses under service state based on the rotating crack model using the concept of average stress and average strain.

2. GOVERNING EQUATIONS

A diagram of a reinforced concrete membrane element subjected to normal stresses is shown in Fig.1(a) where the normal stresses are designated as σ_x and σ_y, and the shear stress as τ_{xy}.

When the principal tensile stress σ_1

reaches the tensile strength of concrete, diagonal cracks will be formed and the concrete will be separated by the diagonal cracks into a series of concrete struts. If the element is reinforced with different amounts of steel in the x and y directions, as shown in Fig.2(c), the direction of the principal stresses in concrete after cracking will deviate from the direction of the applied principal stresses as shown in Fig.2(b).

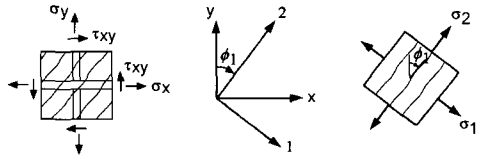

(a) (b) (c)

Fig.1 Definitions of stresses and coordinate system

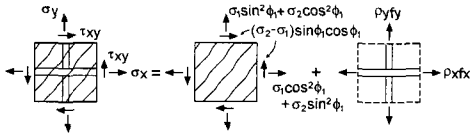

(a) (b) (c)

Fig.2 Stress condition in reinforced concrete element : (a) Reinforced Concrete, (b) Concrete Struts, (c) Reinforcement

The concrete struts are assumed to be oriented in the direction of the postcracking principal compression, designated by the 2-axis as shown in Fig.1(c). Taking the perpendicular direction of principal compression as the 1-axis, we have x, y-coordinate system representing the direction of the postcracking principal stresses and strains in Fig.1(b). The principal compressive stress and the principal tensile stress in the concrete are designated as σ_2 and σ_1, respectively. The x, y-coordinate is oriented at an angle ϕ_1 to the 1,2-coordinate. This angle ϕ_1 is often called the "rotating angle."

2.1 Equilibrium Conditions

The two-dimensional equilibrium condition relates the average internal stresses in the concrete (σ_1, σ_2) and in the reinforcement (f_{sx}, f_{sy}) to the average applied stresses (σ_x, σ_y) on the membrane.

The stresses σ_x, σ_y and τ_{xy} in the reinforced concrete element are resisted by both the concrete and the steel reinforcement. The steel reinforcement is assumed to contribute only axial normal stresses in x and y directions.

The total stress in a reinforced concrete element is the superposition of the concrete stress and the reinforcement contributions

$$\sigma_x = \sigma_1 \cos^2\phi_1 + \sigma_2 \sin^2\phi_1 + \rho_x f_{sx} \quad (1)$$

$$\sigma_y = \sigma_1 \sin^2\phi_1 + \sigma_2 \cos^2\phi_1 + \rho_y f_{sy} \quad (2)$$

$$\tau_{xy} = (\sigma_1 - \sigma_2)\sin\phi_1 \cos\phi_1 \quad (3)$$

where

σ_x, σ_y = normal stresses in the x and y directions, respectively (positive for tension)

σ_1, σ_2 = principal stresses in the 1 and 2 directions, respectively (positive for tension)

ϕ_1 = angle of inclination of the 2-axis with respect to y-axis

ρ_x, ρ_y = reinforcement ratio in x- and y- directions, respectively

f_{sx}, f_{sy} = steel stress in x- and y- directions, respectively

2.2 Compatibility Conditions

The two-dimensional compatibility condition expresses the relationship among the average strains in different coordinate systems. The transformation of average strains between the *x*, *y* coordinate system (ε_x, ε_y, γ_{xy}) and the *1*, *2* principal axes (ε_1, ε_2) gives

$$\varepsilon_x = \varepsilon_1 \cos^2\phi_1 + \varepsilon_2 \sin^2\phi_1 \quad (4)$$

$$\varepsilon_y = \varepsilon_1 \sin^2\phi_1 + \varepsilon_2 \cos^2\phi_1 \quad (5)$$

$$\gamma_{xy} = 2(\varepsilon_1 - \varepsilon_2) \sin\phi_1 \cos\phi_1 \quad (6)$$

$$\varepsilon_x + \varepsilon_y = \varepsilon_1 + \varepsilon_2 \quad (7)$$

where

ε_x, ε_y = average strains in the *x*- and *y*-directions, respectively (positive for tension)

γ_{xy} = average shear strains in *x*-*y* coordinate, respectively

ε_1, ε_2 = average principal strains in the 1-and 2-directions, respectively (positive for tension).

3. LOAD-DEFORMATION RESPONSE OF CRACKED MEMBER

The principles of behavior can be most easily understood by considering the mechanism of cracking of a reinforced concrete member subjected to pure tension.

After the first crack, due to the bond between the steel and concrete, the concrete resists the extension of the reinforcement. Bond stresses, τ_b, are generated to transfer tensile force from the steel to the concrete. In the zones situated close to a crack, the sections behave in a manner intermediate between States I and II. At a certain distance S_{ro} from the first crack, compatibility of strains between the steel and the concrete is re-established. Theoretically, it is only beyond this distance $2S_{ro}$ from the first crack, where the stresses again reach the tensile strength of the concrete, f_{ct}, where a new crack can form.

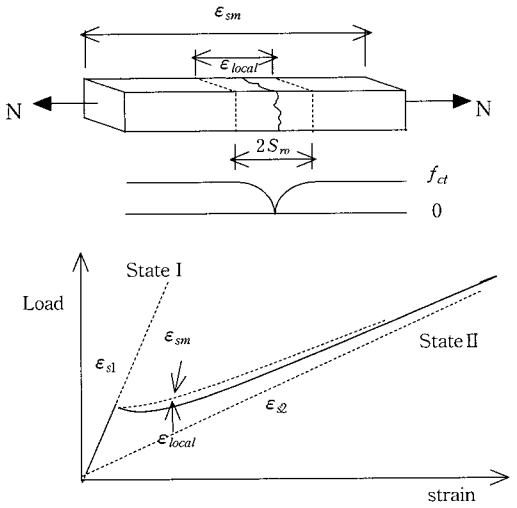

Fig.3 Load-deformation response

The strain in the reinforcement, ε_s, for a tensile force, N, varies between that for State I (ε_{s1}) and that for State II (ε_{s2}). The average strain in the reinforcement, ε_{sm}, can be determined using the provisions of CEB FIP Model Code 78[10]

$$\varepsilon_{sm} = \varepsilon_{s2} \cdot \zeta = \frac{\sigma_s}{E_s}\left[1 - \beta_1\beta_2\left(\frac{\sigma_{sr2}}{\sigma_s}\right)^2\right] \quad (8)$$

where

ε_{s2} = steel strain at cracked section (state II)

ζ = strain reduction factor to allow for the stiffening effects of the concrete in tension

σ_s = steel stress at cracked section (state II)

σ_{sr} =stress in the reinforcement calculated on the basis of a cracked section under the loading conditions causing the first cracking

β_1 = the coefficient which takes into account the bond properties
= 1.0 for high bond bars
= 0.5 for plain bars

β_2 = the coefficient which considers the deterioration of tension stiffening for long term and repeated loading
= 1.0 at the first loading and
= 0.5 for long term or repeated loads independently on their duration

4. CONSTITUTIVE LAW FOR STEEL

The stress-strain relationships of the longitudinal and transverse mild steel can be expressed using elasto-plastic assumption.

$$\varepsilon_x < \varepsilon_{yield} \qquad f_x = E_s \varepsilon_x$$
$$\varepsilon_x > \varepsilon_{yield} \qquad f_x = f_{y,x}$$
$$\varepsilon_y < \varepsilon_{yield} \qquad f_y = E_s \varepsilon_y$$
$$\varepsilon_y > \varepsilon_{yield} \qquad f_y = f_{y,y}$$

where

E_s =modulus of elasticity

$f_{y,x}$, $f_{y,y}$=yield stresses of longitudinal and transverse steel bars, respectively

ε_x, ε_y =yield strains of longitudinal and transverse steel bars, respectively

5. THE REINFORCED CONCRETE MEMBRANE WITH ORTHOGONAL REINFORCEMENT

5.1 The Force Equilibrium in a Reinforced Concrete Membrane Element

The angle of the cracks under service load is denoted by ϕ_1. The forces which act on a unit element of the membrane at the cracks are shown in Fig.4 where A_{sx} and A_{sy} are the areas of reinforcement per unit width in the direction x and y, respectively.

The normal forces acting in the reinforcement at the cracked section in the x and y directions are

$$N_x = \sigma_x \cdot A_{sx} = \sigma_x \cdot \mu_x \cdot h \tag{10}$$

$$N_y = \sigma_y \cdot A_{sy} = \sigma_y \cdot \mu_y \cdot h \tag{11}$$

where $\mu_x = \frac{a_{sx}}{h \cdot 1}$, $\mu_y = \frac{a_{sy}}{h \cdot 1}$

If the angle ϕ_1 is known, the force equilibrium acting on the section parallel to the crack direction can be represented according to Fig.4. The equilibrium equation can be obtained at the cracked section as follows.

$$N_x b_x \cos\phi_1 + N_y b_y \sin\phi_1 = N_1 b_1 \cos(\phi_1 - \alpha) + N_2 b_2 \sin(\phi_1 - \alpha) \tag{12}$$

$$-N_x b_x \sin\phi_1 + N_y b_y \cos\phi_1 = -N_1 b_1 \sin(\phi_1 - \alpha) + N_2 b_2 \cos(\phi_1 - \alpha) \tag{13}$$

The width b_1 to b_y, on which the forces N_1 to N_y are acting, are represented as a function of α and ϕ_1.

The steel forces acting at the cracked section in the x and y directions are

$$N_x = [\cos^2\alpha(1 + \tan\alpha\tan\phi_1)N_1 + \sin^2\alpha(1 - \cot\alpha\tan\phi_1)N_2] \tag{14}$$

$$N_y = [\sin^2\alpha(1 + \cot\alpha\cot\phi_1)N_1 + \cos^2\alpha(1 - \tan\alpha\cot\phi_1)N_2] \tag{15}$$

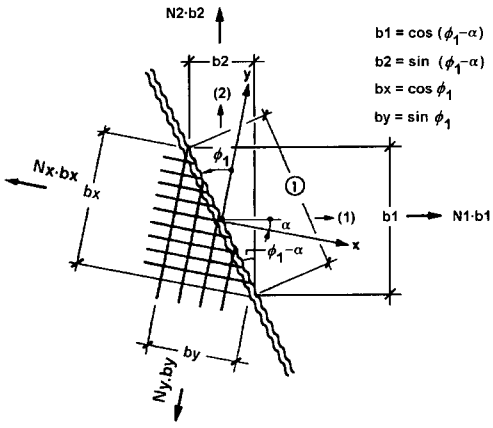

Fig.4 The equilibrium between the external forces and the internal resistance in membrane carrying tension at a cracked section

Thus the average steel forces incorporating the load-deformation response in the x and y directions are

$$N_{sm,x} = N_x - \frac{\beta_1\beta_2\sigma_{sr2,x}^2 A_{sx}^2}{N_x}$$
$$= [\cos^2\alpha(1+\tan\alpha\tan\phi_1)N_1 + \sin^2\alpha(1-\cot\alpha\tan\phi_1)N_2] \quad (16)$$
$$-\left[\frac{\beta_1\beta_2\sigma_{sr2,x}^2 A_{sx}^2}{\cos^2\alpha(1+\tan\alpha\tan\phi_1)N_1 + \sin^2\alpha(1-\cot\alpha\tan\phi_1)N_2}\right]$$

$$N_{sm,y} = N_y - \frac{\beta_1\beta_2\sigma_{sr2,y}^2 A_{sy}^2}{N_y}$$
$$= [\sin^2\alpha(1+\cot\alpha\cot\phi_1)N_1 + \cos^2\alpha(1-\tan\alpha\cot\phi_1)N_2] \quad (17)$$
$$-\left[\frac{\beta_1\beta_2\sigma_{sr2,y}^2 A_{sy}^2}{\sin^2\alpha(1+\cot\alpha\cot\phi_1)N_1 + \cos^2\alpha(1-\tan\alpha\cot\phi_1)N_2}\right]$$

If the unit length normal to the crack direction is considered as shown in Fig.5, the force equilibrium including the diagonal compressive force, D_c, can be obtained.

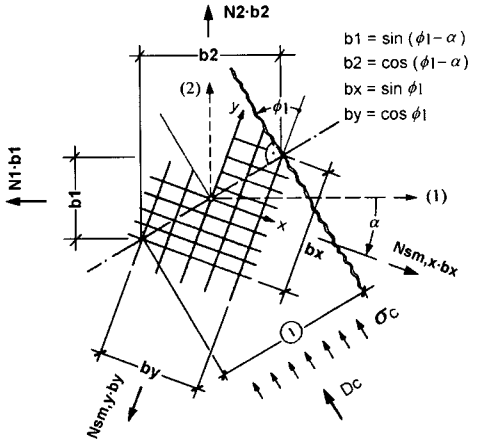

Fig.5 The equilibrium in diagonal compressive strut over unit width between the external forces and the internal resistance

The diagonal compressive force, D_c, is represented from $N_{sm,x}$ and $N_{sm,y}$ as follows

$$D_c = N_{sm,x}\,b_x\sin\phi_1 + N_{sm,y}\,b_y\cos\phi_1 - N_1\,b_1\sin(\phi_1-\alpha) - N_2\,b_2\cos(\phi_1-\alpha)$$
$$= N_{sm,x}\sin^2\phi_1 + N_{sm,y}\cos^2\phi_1 - N_1\sin^2(\phi_1-\alpha) - N_2\cos^2(\phi_1-\alpha) \quad (18)$$

After introduction of $N_{sm,x}$ and $N_{sm,y}$ from eqns. (16),(17) and the given widths b_1 to b_y in Fig.5, the following relationship can be obtained

$$D_c = (N_1 - N_2)\frac{\sin\alpha\cos\alpha}{\sin\phi_1\cos\phi_1} - \left[\frac{\beta_1\beta_2\sigma_{sr2,x}^2 A_{sx}^2\sin\phi_1\cos\phi_1}{(N_1-N_2)\sin\alpha\cos\alpha + (N_1+N_2)\cot\phi_1} + \frac{\beta_1\beta_2\sigma_{sr2,y}^2 A_{sy}^2\sin\phi_1\cos\phi_1}{(N_1-N_2)\sin\alpha\cos\alpha + (N_1+N_2)\tan\phi_1}\right] \quad \cdots\cdots\cdots\cdots (19)$$

5.2 The Crack Direction ϕ_1 in the Elastic Range of the Reinforcement in Both Directions ($\sigma_s < f_y$)

The strain compatibility condition can be used to determine the unknown crack

direction ϕ_1 while ε_x and ε_y can be taken from the average strain concept after cracking as follows

$$\varepsilon_x = \frac{1}{A_{sx}E_s}\left[N_x - \frac{\beta_1\beta_2\sigma_{sr2,x}^2 A_{sx}^2}{N_x}\right]$$
$$= \frac{1}{A_{sx}E_s}\left[\cos^2\alpha(1+\tan\alpha\tan\phi_1)N_1 + \sin^2\alpha(1-\cot\alpha\tan\phi_1)N_2 - \left(\frac{\beta_1\beta_2\sigma_{sr2,x}^2 A_{sx}^2}{\cos^2\alpha(1+\tan\alpha\tan\phi_1)N_1 + \sin^2\alpha(1-\cot\alpha\tan\phi_1)N_2}\right)\right] \quad (20)$$

$$\varepsilon_y = \frac{1}{A_{sx}E_s}\left[N_y - \frac{\beta_1\beta_2\sigma_{sr2,y}^2 A_{sy}^2}{N_y}\right]$$
$$= \frac{1}{A_{sx}E_s}\left[\sin^2\alpha(1+\cot\alpha\cot\phi_1)N_1 + \cos^2\alpha(1-\tan\alpha\cot\phi_1)N_2 - \left(\frac{\beta_1\beta_2\sigma_{sr2,y}^2 A_{sy}^2}{\sin^2\alpha(1+\cot\alpha\cot\phi_1)N_1 + \cos^2\alpha(1-\tan\alpha\cot\phi_1)N_2}\right)\right] \quad (21)$$

Minimum principal strain, ε_2, can be obtained from the diagonal compressive force parallel to the crack direction

$$\varepsilon_2 = -\frac{D_c}{h\cdot E_c}$$
$$= -\frac{1}{h\cdot E_c}\left[(N_1-N_2)\frac{\sin\alpha\cos\alpha}{\sin\phi_1\cos\phi_1} - \left(\frac{\beta_1\beta_2\sigma_{sr2,x}^2 A_{sx}^2 \sin\phi_1\cos\phi_1}{(N_1-N_2)\sin\alpha\cos\alpha + (N_1+N_2)\cot\phi_1} + \frac{\beta_1\beta_2\sigma_{sr2,y}^2 A_{sy}^2 \sin\phi_1\cos\phi_1}{(N_1-N_2)\sin\alpha\cos\alpha + (N_1+N_2)\tan\phi_1}\right)\right] \quad \cdots\cdots\cdots\cdots (22)$$

Maximum principal strain, ε_1, from the compatibility condition is

$$\varepsilon_1 = \varepsilon_x + \varepsilon_y - \varepsilon_2 \quad (23)$$

The compatibility condition and eqns(20),(21),(22),(23) yield the following equation to take the crack direction ϕ_1 under service state.

$$\varepsilon_1\cos^2\phi_1 + \varepsilon_2\sin^2\phi_1 - \varepsilon_x = 0 \quad (24)$$

Introducing the new variables;

k: the ratio of minimum principal force and maximum principal force $\left(\frac{N_2}{N_1}\right)$

l : $N_1(N_1-N_2)$

m: $N_1(N_1+N_2)$

λ : ratio of reinforcement contents $\left(\frac{A_{sx}}{A_{sy}} = \frac{\mu_{sx}}{\mu_{sy}}\right)$

ν : ratio of the stiffness of reinforcement (x)and the modulus of elasticity of the concrete $\left(\mu_{sx}\cdot\frac{E_s}{E_c}\right)$

After some transformations of Eqn.(24), the following equation for the crack direction under the service state can be obtained.

$$\cot^4\phi_1\left(1+\frac{\nu}{\lambda}\right) + \cot^3\phi_1\frac{(\tan\alpha + k\cot\alpha)}{(1-k)} - \cot\phi_1\frac{(\cot\alpha + k\tan\alpha)}{\lambda(1-k)} - \frac{1}{\lambda}(1+\nu) + \frac{\beta_1\beta_2\sigma_{sr2,x}^2 A_{sx}^2\cot^2\phi_1}{\lambda\sin\alpha\cos\alpha(1-k)(l\sin\alpha\cos\alpha + m\cot\phi_1)}\cdot\left[\frac{(1+\nu)+(1-\nu)\cot^2\phi_1}{1+\cot^2\phi_1}\right] + \frac{\beta_1\beta_2\sigma_{sr2,y}^2 A_{sy}^2\cot^2\phi_1}{\lambda\sin\alpha\cos\alpha(1-k)(l\sin\alpha\cos\alpha + m\tan\phi_1)}\cdot\left[\frac{(\nu-\lambda)-(\nu+\lambda)\cot^2\phi_1}{1+\cot^2\phi_1}\right] = 0 \quad \cdots\cdots\cdots\cdots (25)$$

The positive real root of this equation gives the angle ϕ_1 of crack direction under service state when the reinforcement stress(σ_s) is below the yield strength(f_y). This crack direction is dependent on the ratio of reinforcement contents, the ratio of maximum principal force and minimum principal force, and the reinforcement

direction in the membrane element.

6. COMPARISON OF THEORETICAL RESULTS WITH EXPERIMENTAL RESULTS

The response of reinforced concrete panels subjected to in-plane shear and normal stresses have been extensively investigated by Vecchio and Collins[6] and Hsu and Pang[9].

6.1 Comparison with Vecchio & Collins' Results

Vecchio and Collins tested the reinforced concrete panels of 890x890x70[mm] reinforced with welded wire mesh[6]. The plan view of reinforcing steel and loading directions are shown in Fig.6.

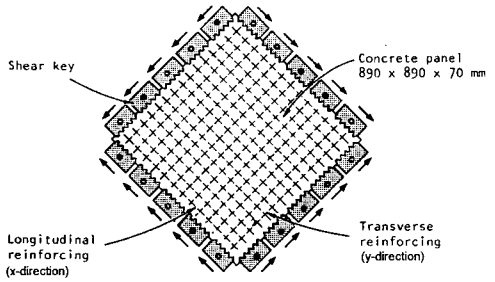

Fig.6 The specimens and loading directions tested by Vecchio and Collins

A list of the analyzed panels with concrete properties and reinforcement contents are given in Table 1.

The pattern of cracking under service state of the test panels PV10, PV11, PV19, and PV20 under pure shear ($N_1 = -N_2$) are compared with the proposed crack direction under service state in Fig.7 to Fig.10.

Table 1 Material properties for Vecchio and Collins specimens

panel	concrete		reinforcement			
	f_c' MPa	ε_0	content ratio		yield strength MPa	
			ρ_x	ρ_y	$f_{y,x}$	$f_{y,y}$
PV10	14.5	0.00270	0.01785	0.00999	276	276
PV11	15.6	0.00260	0.01785	0.01306	235	235
PV19	19.0	0.00215	0.01785	0.00713	458	299
PV20	19.6	0.00180	0.01785	0.00596	460	297

The panel PV10 shows the failure mode of steel yielding, but panels PV11, PV19, and PV20 show the mode of concrete shear failure.

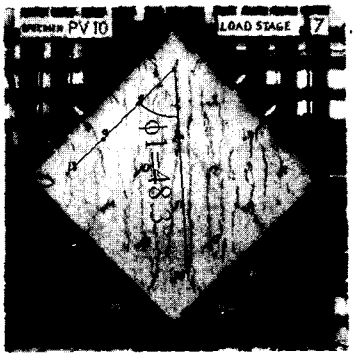

Fig.7 PV10(v=3.97 MPa)

Fig.8 PV11(v=3.52 MPa)

Fig.9 PV19 (v=3.72 MPa)

Fig.10 PV20 (v=4.26 MPa)

The crack directions by proposed theory are 48.3° in PV10, 46.7° in PV11, 50.1° in PV19, and 49.0° in PV20 respectively which show good agreement with experimental results.

The load-deformation responses of the membranes are shown in Fig.11- Fig.14.

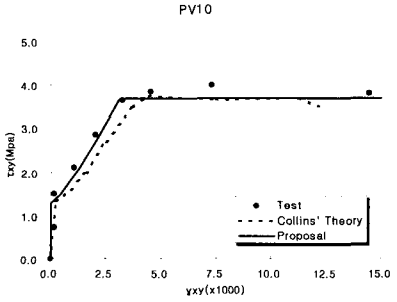

Fig.11 PV10

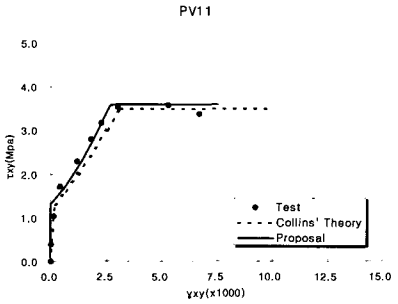

Fig.12 PV11

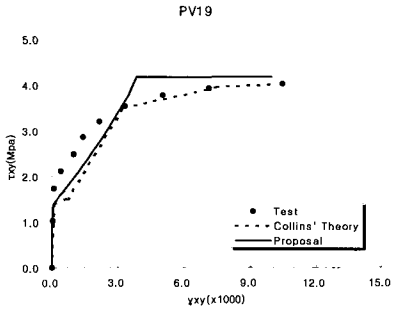

Fig.13 PV19

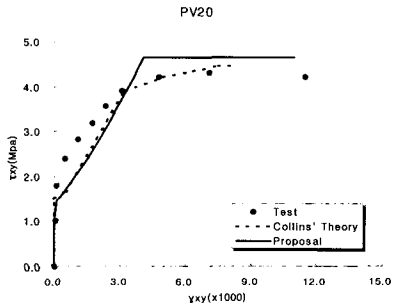

Fig.14 PV20

Although the response of PV10 and PV11 show good agreement, the response of PV19 and PV20 overestimate shear strain γ_{xy} compared with test results. It is possible that the secondary effect of aggregate interlock or kinking effect which we have not considered take some role.

6.2 Comparison with Hsu & Pang's Results

The reinforced concrete panels of $55x55x7^{in}$ were tested by Hsu and Pang[9]. Reinforcement was arranged at 45 deg., with respect to the applied loading directions as shown in Fig.15.

Concrete strength, yield stress of reinforcement, and the ratio of reinforcement contents of the panels are listed in Table 2 by Hsu and Pang.

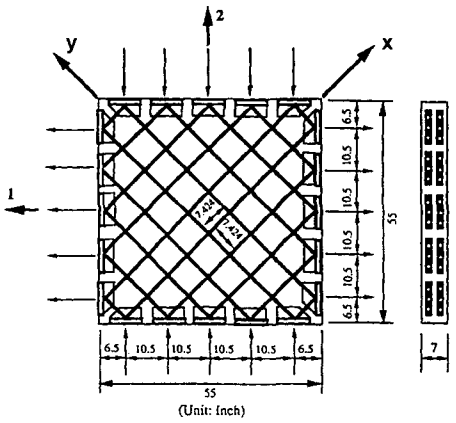

Fig.15 The reinforcement arrangement and loading directions tested by Hsu and Pang

Table 2 Material properties for Hsu and Pang specimens

panel	concrete		Reinforcement			
	f_c' ksi	ε_0	content ratio		yield strength ksi	
			ρ_x	ρ_y	$f_{y,x}$	$f_{y,y}$
A2	5.98	0.00210	0.01193	0.01193	67.10	67.10
A3	6.04	0.00194	0.01789	0.01789	64.75	64.75
B2	6.39	0.00235	0.01789	0.01193	64.75	67.10
B3	6.51	0.00215	0.01789	0.00596	64.75	64.51
B5	6.21	0.00220	0.02982	0.01193	68.13	67.10
B6	6.23	0.00220	0.02982	0.01789	68.13	64.75

The theoretical shear strains are compared with experimental shear strains under the incremental monotonic shear load($N_1 = -N_2$) in Fig.16 to Fig.21.

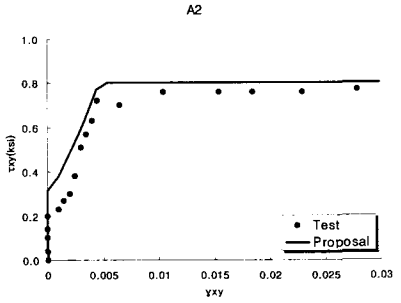

Fig.16 A2

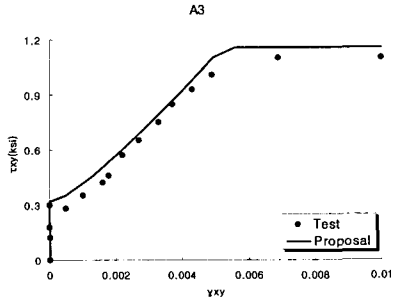

Fig.17 A3

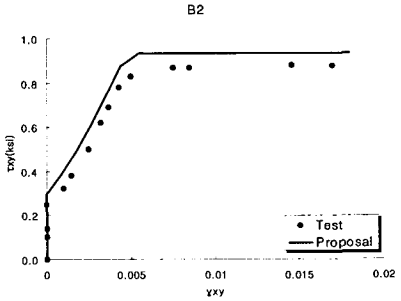

Fig.18 B2

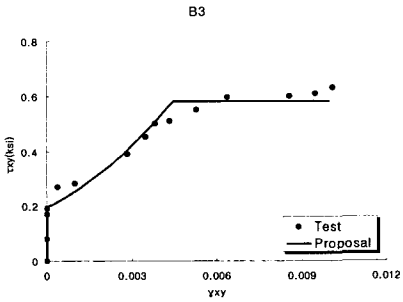

Fig.19 B3

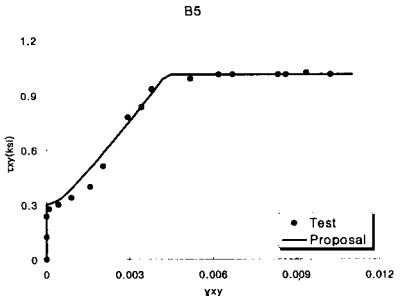

Fig.20 B5

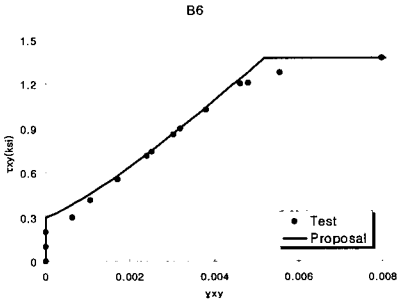

Fig.21 B6

Panels A2 and A3, and B2, B3, B5 and B6 fail by steel yielding.

Yield plateau is determined simply from the equilibrium condition when one of the reinforcement in x and y direction reaches the yield stress (f_y).

In general, a good agreement is obtained between the experimental strains and the proposed strains on the basis of the rotating crack model under service state.

7. CONCLUSION

A theory based on the rotating crack model is proposed from equilibrium, compatibility conditions, load-deformation response of cracked member as well as constitutive law for material to obtain the crack direction and the shear load-deformation response of reinforced concrete membrane element under service state.

1. The unknown crack directions can be directly determined by the equation proposed on the basis of the equilibrium and the compatibility conditions, which show good agreement with the experimental results under service state.
2. The tension stiffening effect in reinforced concrete structures can be taken into account by incorporating the average tensile stress-strain relationship of cracked concrete members.
3. The shear load-deformation response by the proposed theory shows good agreement with test results.

This theory is applicable to predict the service state behavior of a variety of concrete structures subjected to shear, such as shear walls, deep beams, containment structures, and offshore platforms.

ACKNOWLEDGMENT

This research was sponsored by Dong-A University. This generous supports are gratefully acknowledged.

REFERENCES

1. Gupta, A.K., and Akbar, H., "Cracking in Reinforced Concrete Analysis," Journal of Structural Engineering, ASCE, V.110, No.8, Aug. 1984, pp.1735-1746.
2. Kollegger,J., "Ein Materialmodell für die Berechung von Stahlbetonflächentragwerken," Dissertation, Gesamthochschule Kassel, 1988, Germany.
3. Crisfield, M.A. and Wills, J.,"Analysis of R/C panels using different concrete models," Journal of Engineering Mechanics, ASCE, 155(3), 1989, pp.578-597.

4. Vecchio, F.J. and Collins, M.P., "The Modified Compression-Field Theory for Reinforced Concrete Elements Subjected to Shear," ACI Journal, V.83, No.2, Mar.-Apr., 1986, pp.219-231.
5. Hsu, Thomas, "Nonlinear Analysis of Concrete Membrane Elements," ACI Structural Journal, V.88, No.5, Sep.-Oct. 1991.
6. Vecchio, F.J. and Collins, M.P., "Response of Reinforced Concrete to In-Plane Shear and Normal Stresses," Publication 82-03, Dept of Civil Engineering, University of Toronto, Toronto, Canada, 1982, 332 pp.
7. Bhide, S.B. and Collins, M.P., "Reinforced concrete elements in shear and tension," Publication 87-02, University of Toronto, Canada, 1987.
8. Kollegger,J. and Mehlhorn, G., "Experimentelle Untersuchungen zur Bestimmung der Druckfestichkeit des gerissenen Stahlbetons bei einer Querzugbeanspruchung," Heft 413, Deutscher Ausschuß für Stahlbeton, Germany, 1990.
9. Hsu, Thomas and Pang, "Behavior of Reinforced Concrete Membrane Elements in Shear," ACI Structural Journal, V.92, No.6, Nov.-Dec. 1995.
10. CEB FIP Model Code 78, 1978.